Applied Catalysis B: Environmental 88 (2009) 533–541

Contents lists available at ScienceDirect

Applied Catalysis B: Environmental

journal homepage: www.elsevier.com/locate/apcatb

Stability of protonic zeolites in the catalytic oxidation of chlorinated VOCs (1,2-dichloroethane)

A. Aranzabal [a,*], J.A. González-Marcos [a], M. Romero-Sáez [a], J.R. González-Velasco [a], M. Guillemot [b], P. Magnoux [b]

[a] Group "Chemical Technologies for Environmental Sustainability" Chemical Engineering Department, Faculty of Sciences and Technology, Universidad del País Vasco/EHU; P.O. Box 644, E-48080 Bilbao, Spain

[b] Laboratoire de Catalyse en Chimie Organique, UMR 6503, Université de Poitiers, 40, Avenue du Recteur – Pineau, 86022 Poitiers Cedex, France

ARTICLE INFO

Article history:
Received 30 May 2008
Received in revised form 10 October 2008
Accepted 18 October 2008
Available online 28 October 2008

Keywords:
Catalytic oxidation
1,2-Dichloroethane
H-zeolite catalysts
Deactivation
Space velocity
Temperature
H_2O
HCl

ABSTRACT

The deactivation of protonic zeolites in the catalytic oxidation of 1,2-dichloroethane (DCA) was evaluated. DCA oxidation reactions were carried out in a conventional fixed-bed reactor at atmospheric pressure under conditions of lean DCA concentration in air (1000 ppm). The outlet composition was analysed by a gas chromatograph, an IR spectroscopy-based analyser and another UV analyser. The effect of the zeolite crystalline structure was examined in order to track the catalytic stability of H-ZSM-5, H-MOR and H-BEA under typical reaction environment and conditions (1000 ppm DCA, 300 °C, 13,500 h^{-1}). With the aim of a better understanding of the deactivation pathway, the influence of the space velocity and temperature on the durability of protonic zeolites was analysed. Since some products formed during reaction could also cause deactivation, H_2O and HCl were introduced in the feed stream along with the DCA itself, so as to evaluate their effect. In general terms, coke formation was concluded to be the main reason for zeolite catalyst deactivation. Coke was formed from the intermediate vinyl chloride (VC), which resulted from a first dehydrochlorination step of DCA.

1. Introduction

Chlorinated volatile organic compounds (CVOCs) such as 1,2-dichloroethane (DCA) constitute a significant fraction of the hazardous air pollutants due to their inertness and their widespread application in industry [1]. One of the major stationary sources of VOC emissions is the usage of solvents, emissions of which are limited in EU countries by the Solvent Emissions Directive [2]. Among the several disposal methods for those molecules, low-temperature catalytic oxidation has recently gained interest due to its low operational cost [3–6]. The desired reaction is the complete oxidation of the chlorinated VOC to produce HCl, CO_2 and H_2O. Our previous researches [7,8] as well as others reported in the literature [9,10] showed H-zeolites, such as H-ZSM-5, H-MOR and H-BEA, as potential catalysts for end-of-pipe pollution control, because of their high activity and selectivity towards desired reaction products. Nevertheless, in industrial applications, catalyst stability and durability are as important as their activity and selectivity, as these properties have to keep constant with reaction time in order to fulfil international environmental regulations and to be economically more attractive.

Indeed, over the past three decades, the science of catalyst deactivation has been steadily developing, while literature addressing this topic has expanded considerably to include books [11–13]; comprehensive reviews [14–17]; and proceedings of international symposia [18,19]. However, literature about the deactivation of catalysts employed in the oxidation of VOCs is rather limited, especially when they are halogenated.

The deactivation may be caused by several reasons, both physical and chemical, depending on the process where the catalyst is used [20]. The main deactivation mechanisms over oxidation catalysts in solvent emission abatement are most probably fouling and chemical deactivation, although thermal shocks and abrasion of the catalytic surface may occur. Libanati et al. [21] studied silica poisoning of bead VOC catalysts in industrial-scale oxidation of printing emissions and found out that silica penetrated into the catalyst bed and deposited in the micro pores of the catalyst. Vigneron et al. [22] tested several different catalysts (in shape and in composition) in the abatement of VOC emissions originating from a coil-coating process. They reported

* Corresponding author. Tel.: +34 946015554; fax: +34 946013500.
E-mail address: asier.aranzabal@ehu.es (A. Aranzabal).

0926-3373/$ – see front matter © 2008 Elsevier B.V. All rights reserved.
doi:10.1016/j.apcatb.2008.10.007

poisoning by silicone and deactivation due to thermal stress as well as attrition. Agarwal et al. [23] noted that chlorinated feeds caused more deactivation on a commercial chromia-alumina catalyst. Rachapudi et al. [24] reported the deactivation pathway for the a chromium exchanged ZSM-5 catalysts during oxidative destruction of 1% vinyl chloride or trichloroethylene involved slow generation of volatile CrO_2Cl_2 which caused cation migration and loss. Guillemot et al. [25] also reported attack of HCl formed during oxidation of tetrachloroethylene over Pt/HY, Pt/NaY and Pt/NaX. Chatterjee et al. [26] reported formation of coke as the main reason for the deactivation of metal exchanged zeolites in the oxidation of several chlorinated VOC.

Nevertheless, for most catalysts the activity declines sharply at first and then reaches a state where the catalyst activity decreases much more slowly with time, and the selectivity associated with the activity change may improve or become worse.

The aim of this work is to analyse the stability and durability of H-zeolites (H-ZSM-5, H-MOR and H-BEA) in the oxidation of 1,2-dichloroethane under typical off-gases conditions. Previous research carried out by our research group [7,8] about activity and selectivity has shown good performance of this zeolites. 1,2-Dichloroethane is a typical solvent commonly appearing in industrial waste streams, such us in vinyl chloride monomer plants [4] and groundwater air-stripping emissions admixtured with other chlorinated solvents such as trichloroethylene, dichloromethane and 1,2-dichloroethylene [23].

2. Experimental

2.1. Preparation and characterization of the catalyst

The reaction was carried out over three different H-zeolite catalysts: H-ZSM-5 (Si/Al molar ratio of 25), H-BEA (Si/Al molar ratio of 12.5) and H-MOR (Si/Al molar ratio of 6.5) supplied by Zeolyst International. These samples were calcined in air at 550 °C for 3 h and then pelletised under 29 kN during 3 min (Specac hydraulic press). The resulting pellets were crushed and sieved to a particle size of 0.3–0.5 mm. Before the reaction run, zeolite catalysts were dried at in the reactor itself under a 500 $cm^3\ min^{-1}$ stream of dry air at 150 °C for 2 h.

The BET surface areas and pore volumes of the zeolite samples were determined by N_2 adsorption–desorption at −196 °C in a Micromeritics ASAP 2010 equipment.

Temperature-programmed desorption (TPD) of ammonia was performed on a Micromeritics AutoChem 2910 instrument. Prior to adsorption experiments, the samples (30–40 mg) were first pre-treated in a quartz U-tube in a nitrogen stream at 500 °C. Then, they were cooled down at 100 °C in a N_2 flow (20 $cm^3\ min^{-1}$) before the ammonia adsorption started. The adsorption step was performed by admitting small pulses of ammonia in Ar at 100 °C up to saturation. Subsequently, the samples were exposed to a flow of argon (50 $cm^3\ min^{-1}$) for 2 h at 100 °C in order to remove reversibly and physically bound ammonia from the surface. Finally, the desorption was carried out from 100 to 500 °C at a heating rate of 10 °C per min in an Ar stream (50 $cm^3\ min^{-1}$). This temperature was maintained for 15 min until the adsorbate was completely desorbed. The amount of ammonia desorbed at a given temperature range was taken as a measure of the acid site concentration, whereas the temperature range at which most of the ammonia was desorbed indicated the acid strength distribution [27,28]. All the samples showed two major desorption peaks (Fig. 1): A desorption peak around 180–200 °C was considered as corresponding to weak acid sites, while the peak in the range 350–450 °C was considered as corresponding to strong acid sites. The profiles were simulated according to two Gaussian functions

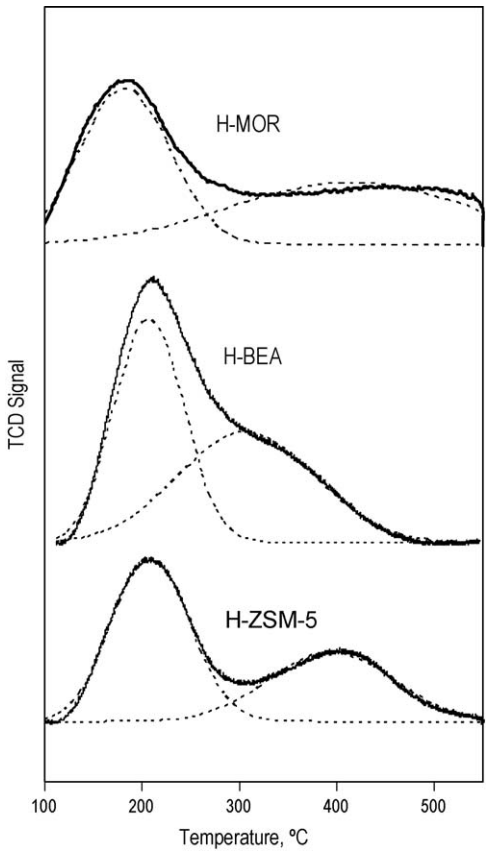

Fig. 1. TPD of ammonia spectra from H-ZSM-5, H-BETA and H-MOR fresh zeolites.

associated with the desorption at low and high temperatures, respectively [29], as shown in Fig. 1. The fitting quality of the deconvolution, measured as correlation coefficient (R^2) of least square fiiting, was always higher than 0.997 for H-BEA and H-ZSM-5 and 0.988 for H-MOR.

The X-ray powder diffraction (XRD) patterns for the measurement of the zeolite crystallinity, were recorded on a Philips PW 1710 X-ray diffractometer with Cu Kα radiation and Ni filter.

Coke content was also measured by heating the spent catalysts up to 850 °C at 5 °C min^{-1} under synthetic air flow (300 N $cm^3\ min^{-1}$, 100 kPa) in a thermogravimetric analyser (Hiden Analytical IGA-003). The composition of coke was determined according to Guisnet and Magnoux [30,31], i.e. dissolution of the zeolite in hydrofluoric acid and recovery of the coke molecules in two parts, one soluble in methylene chloride and the other insoluble; this latter is generally composed of highly polyaromatic compounds. Coke soluble in methylene chloride was analysed by GC/MS.

2.2. Experimental set-up

The experimental set-up is shown in Fig. 2. The feed consisted of a dry compressed air stream, whose flow rate was regulated by a gas mass flow controller (Bronkhorst Hi-Tec El-Flow), and of two liquid streams of DCA and H_2O, respectively, which were dosed by two liquid mass flow controllers (Bronkhorst Hi-Tec μ-Flow). The three streams were blended in a controlled-evaporator-mixer (Bronkhorst Hi-Tech), which evaporated and homogenized the mixture. The resulting gaseous stream crosses the fixed catalytic bed inside a tubular quartz reactor, which was surrounded and heated by a convective-flow oven. Then, the reactant and products were dried by a permeation system (Permapure dryer) using dry

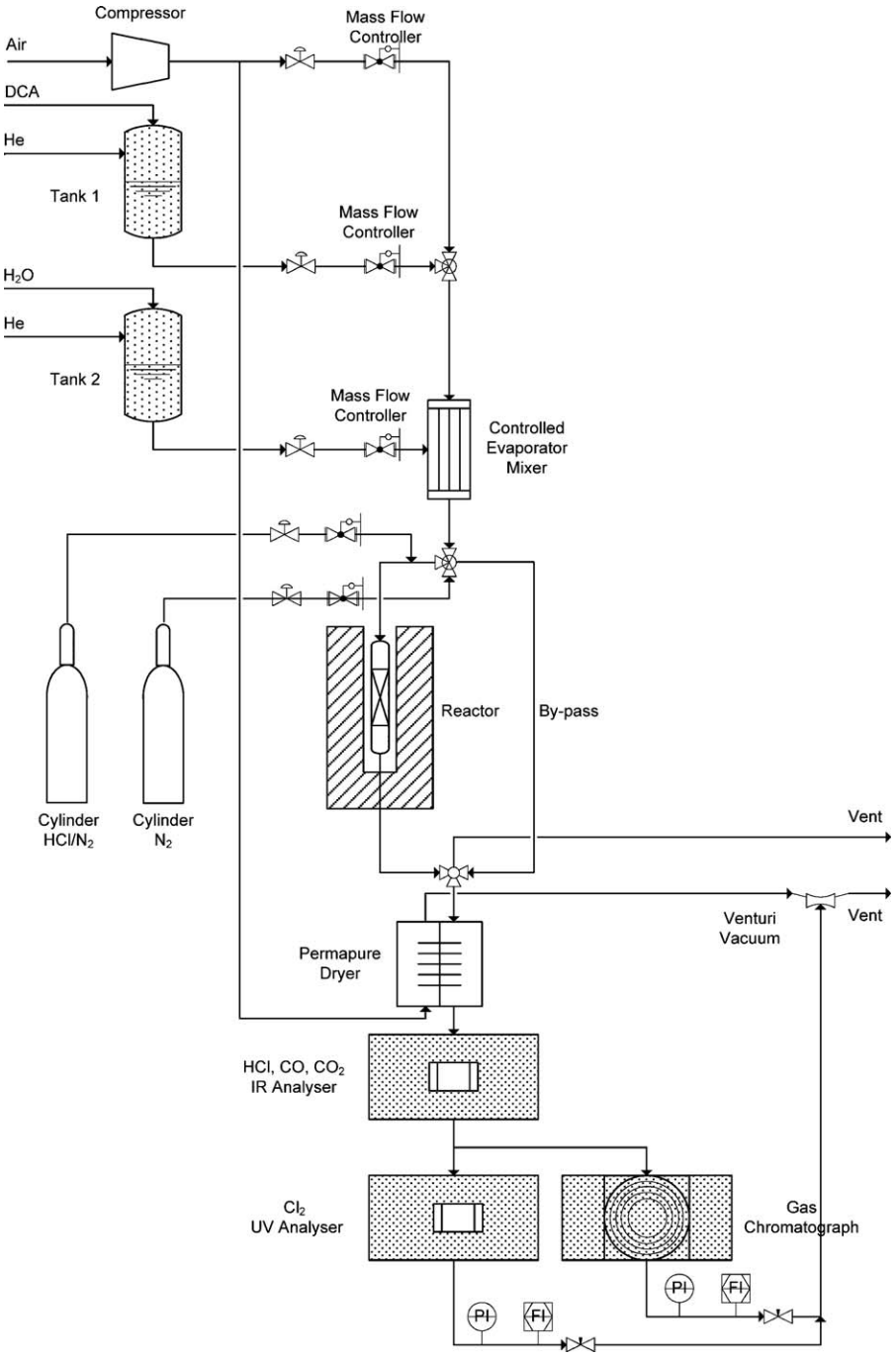

Fig. 2. The experimental set-up.

air in counter current and finally were directed towards an on-line analysis system. This system consisted of an analyser based on infrared spectroscopy (Environnement MIR-IS) to measure the concentrations of HCl, CO and CO_2, another ultraviolet-based analyser (Emerson Rosemount MLT2) to measure Cl_2, and a gas chromatograph (Agilent Technologies 6890N) equipped with a HP-5 capillary column and an electron capture detector (μ-ECD) detector to separate and measure chlorinated hydrocarbons.

2.3. Experimental conditions

The deactivation was studied by following the activity in terms of DCA conversion as a function of time-on-stream over different zeolites and under different reaction conditions. Catalytic oxidation reactions were carried out feeding 1000 ppmv of DCA at atmospheric pressure. Space velocity was varied between 6000 h^{-1} (300 N cm^3 min^{-1} air flow rate, 1.33×10^{-3} g min^{-1} liquid DCE rate, 1.275 g catalyst) and 13,500 h^{-1} (450 N cm^3 min^{-1} air flow rate, 2.00×10^{-3} g min^{-1} liquid DCE rate, 0.850 g catalyst) and the temperature was varied between 270 °C and 300 °C.

On the other hand, the effect of HCl and water were analysed by adding to the feed stream 700 ppmv of HCl and 10,000 ppmv of H_2O, respectively. There experiments were carried out by adding to the main feed stream 20 N cm^3 min^{-1} of HCl additive (0.16% HCl/N_2 mixture) supplied through a Cole-Parmer 65 mm Correlated PTFE Flowmeter with valve (EW-03216-67) and mixed at the

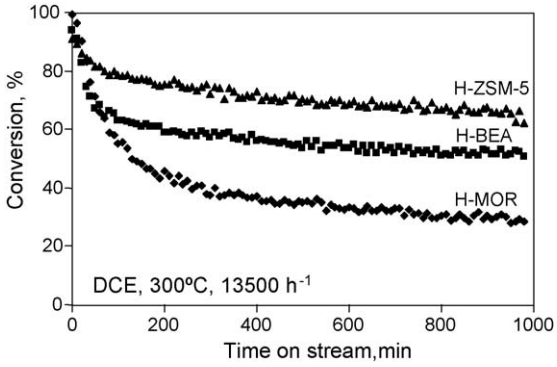

Fig. 3. Catalytic activity of different zeolite structures as a function of time on stream (H-ZSM-5, H-MOR and H-BEA) at 300 °C and 13,500 h^{-1}.

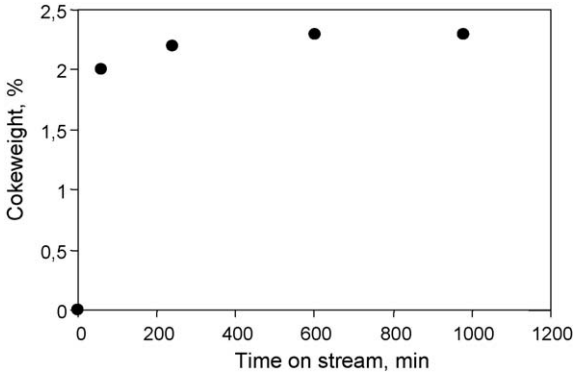

Fig. 4. Coke formation along reaction time (H-ZSM-5, 13,500 h-1, 300 °C, 1000 ppm DCA).

reactor inlet with 254 N cm^3 min^{-1} of air premixed with DCE (2.00×10^{-3} g min^{-1}), in order to maintained 1000 ppm of DCE. Similarly, the experiments to analyse the effect of the water were made by adding 0.144 g h^{-1} of liquid water through mass flow controllers as described above.

These experimental conditions were chosen on the basis of previous experience so as to prevent from mass transfer limitation. In any case, mass transfer effects were evaluated to ensure that kinetic experiments were carried out under conditions free of diffusional resistances, according to the procedure described elsewhere [32]. No transport effects were found.

3. Results and discussion

3.1. Effect of the zeolite structure on the catalytic stability

Fig. 3 shows the behaviour of H-zeolites in the oxidation of DCA as conversion vs. time on stream. Conversion fell rapidly in the initial stages of the reactions and tended to stabilise for longer times. H-MOR was the most active catalyst (conversion: 99%) as the operation started, followed by H-BEA (94%) and H-ZSM-5 (91%); however, after 16 h the stability of the zeolites followed the order: H-ZSM-5 (conversion: 66%) >H-BEA (52%) >H-MOR (30%).

Characterisation results are summarised in Table 1 for the fresh and aged catalysts. Their BET surface area, pore volume, total acidity underwent a remarkable decrease, indicating that the zeolites were deactivated in some extent, which could be caused by coke deposition, as measured by elemental analysis.

N_2 physisorption results indicated that H-ZSM-5 had the smallest decrease in the BET surface area compared to H-BEA and H-MOR, though differences were not significant. Microporosity was decrease also in similar extent as BET surface. H-BEA possesses a large amount of mesopores due to its inter-crystalline volume, which were reduced in 20%.

According to the total acidity, H-MOR zeolite has initially more acid sites than H-ZSM-5 and H-BEA. Previous researches carried out by modifying the acidity of the zeolites by chemical dealumination [7,8], revealed that strong Brønsted acidity plays an important role in controlling the oxidative activity of the H-type zeolites.

After 16 h of operation at 300 °C, 13,500 h^{-1} and 1000 ppm DCA feed, the reduction in the total number of acid sites in H-ZSM-5 was lower than in HBEA and H-MOR, respectively. The order in reduction of total acidity (H-ZSM5, 9% <H-BEA, 17%, <HMOR, 29%) was the same as order in conversion decay (H-ZSM5, 28% <H-BEA, 42%, <HMOR, 70%). This correlation suggested that acidity plays important role in the activity of the zeolites.

Comparing the amounts of coke in weight percent, the value for H-BEA was higher than for H-ZSM-5 and H-MOR. Fig. 4 shows the rate of coke formation during reaction time. Coke was rapidly formed within the first 60 min and then the rate of formation was reduced and tended to zero. This profile coincides with the conversion profiles showed in Fig. 3.

The crystallinity of the aged zeolites practically was not affected, except for H-BEA, whose crystallinity presented a slight decrease with respect to the fresh sample, although this effect was not significant.

According to the pore structure of the selected zeolites, the initial loss of activity is due to coke formation on strong acid sites. It is generally believed that coking mainly occurs inside the zeolite pores and affects the activity of zeolites in two different ways: site coverage (active sites poisoned by coke adsorption) and pore blockage (active sites inaccessible to reactants) [33,34]. The pore structure also governs the rate of diffusion of organic molecules

Table 1
Physico–chemical properties for the fresh and aged H-zeolite catalysts.

	S_{BET}, (m^2 g^{-1})	V_{micro}, (cm^3 g^{-1})	V_{meso}, (cm^3 g^{-1})	Total acidity, (mmol NH_3 g^{-1})	Weak acidity, (mmol NH_3 g^{-1})	Strong acidity, (mmol NH_3 g^{-1})	Crystallinity, (%)	Coke content, (%)
H-ZSM-5, fresh	411	0.17	0.08	0.286	0.103	0.183	–	–
H-ZSM-5, 13,500 h^{-1}, 270 °C	350	0.14	0.08	0.103	0.039	0.064	95	1.4
H-ZSM-5, 13,500 h^{-1}, 300 °C	336	0.14	0.08	0.261	0.098	0.163	100	2.3
H-ZSM-5, 6000 h^{-1}, 300 °C	314	0.13	0.07	0.146	0.027	0.119	99	2.8
H-MOR, fresh	412	0.19	0.04	0.627	0.324	0.303	–	–
H-MOR, 13,500 h^{-1}, 270 °C	350	0.16	0.05	0.124	0.029	0.094	97	2.2
H-MOR, 13,500 h^{-1}, 300 °C	322	0.15	0.06	0.446	0.208	0.238	99	2.2
H-MOR, 6000 h^{-1}, 300 °C	336	0.16	0.05	0.322	0.125	0.197	94	2.5
H-BEA, fresh	520	0.22	0.55	0.316	0.160	0.156	–	–
H-BEA, 13,500 h^{-1}, 270 °C	458	0.19	0.49	0.215	0.042	0.173	87	3.0
H-BEA, 13,500 h^{-1}, 300 °C	400	0.17	0.44	0.261	0.104	0.158	89	3.4
H-BEA, 6000 h^{-1}, 300 °C	426	0.18	0.46	0.249	0.144	0.105	84	3.6

inside the zeolite, which depends on the length, size of pore apertures and of channel intersections, channel tortuosity and acid site density. The slower the diffusion of the organic molecules, the higher the contact time with acid sites and the greater the coking rate. H-ZSM-5 and H-BEA zeolites have an interconnected three-dimensional channel system, whereas H-MOR has a one-dimensional pore structure.

Although H-MOR is the zeolite with highest acidity and then highest initial activity, the diffusion of reactants to the acid sites is hindered because the one-dimensional pore structure, so small amount of coke is enough to deactivate the zeolite.

Zuhairi et al. [35] reported that relatively large pore size (6.6 × 6.7 Å) channel system in H-BEA makes it prone to coking because bulky molecules may be trapped within and end up as coke deposits. Although H-BEA presented higher coke content than H-MOR, the greater stability of H-BEA is due to its three-dimensional pore system and higher mesoporosity. The lower rate of deactivation in H-ZSM-5 can be related to its three-dimensional channel structure, the uniform channel size (5.1 × 5.5 Å), interconnecting channels and the absence of bottlenecks, which easily allows the inlet of feed molecules as well as the outlet of the product molecules.

The rate of acid catalysis reactions is determined by the characteristics of the acid sites. The rate of hydrocarbon transformations (and coking is of this type) depends essentially on the strength and on the total number of the acid sites. Guisnet et al. [34] pointed out that the greater the number of acid sites the higher the coking rate, since coke formation demands a large number of successive reactions. On the other hand the stronger the acid sites the stronger the adsorption of the reactant, hence the longer the contact time and the more significant the secondary reactions leading to coke formation. López-Fonseca et al. [36,37] revealed that strong Brönsted acidity plays a key role in determining the zeolite activity in this type of reactions. Guisnet et al. [34] stated that the deactivating effect of coke molecules is initially very high because coke molecules are formed on the strongest (thus the most active) acid sites. This can explain rapid conversions fall in the initial stages of the reactions and the trend to stabilise for longer times.

The deactivating effect of coke can be explained by the following mechanisms: on H-ZSM-5 a competition for adsorption on the acid sites between the reactant and the coke molecules may happen. For H-BEA site coverage by coke may render the active sites inaccessible to reactants by coke deposits. Then, activity decrease is higher. In the case of H-MOR, pore blockage may occur, instead of site coverage, which involves a more pronounced deactivation [34]. In this case a small amount of coke is enough to deactivate the zeolite.

3.2. Effect of space velocity on catalyst deactivation

The operating conditions must be chosen carefully to avoid secondary reactions leading to coke maker molecules such as alkenes. The coking rate depends also on the reaction conditions, therefore, the influence of the space velocity and temperature on the deactivation of these zeolites [26,33] was analysed.

In order to see the effect of the space velocity on the deactivation, Fig. 5 shows the conversion vs. time on stream for the three zeolites at 13,500 and 6000 h^{-1} and 300 °C. It was observed that when decreasing space velocity, thus increasing space time, the activity drop was smaller for all the three catalysts.

From Table 1 it could be concluded that the BET surface area decrease was lower for high space times, but total acidity along with crystallinity diminished with space time. XRD data showed a slight decrease in the crystallinity of the zeolites at highest space time. The coke contents slightly increased (between 6% and 18%) with the space time. It was concluded that coking process was enhanced with the space time.

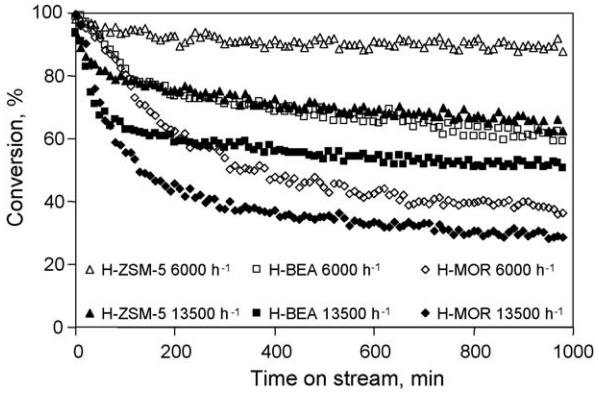

Fig. 5. Effect of different space velocities on the catalytic activity at 300 °C, as a function of time on stream.

The coke formation profile along the catalyst bed was measured both by photographing (Fig. 6) and by thermogravimetric analysis of segmented bed (Table 2). The darker zone corresponded to coked zeolite. These results showed that the coke weight profile decreased with the distance from the inlet, suggesting that coking results from a reactant or an intermediate formed early in the oxidation of DCA.

By assuming that coking would occur in a reaction either in parallel or consecutive to the main reaction, the profile of deposited coke would provide information about coke forming mechanism [38]. When coking occurs by a parallel mechanism (coke is formed from reactants), the greatest deposition of coke would be expected at the inlet of the reactor. Conversely, when products are the precursor of the coke, named series coking mechanism, concentration of coke is increased with distance along the catalytic bed.

The analysis of the product distribution in the DCA catalytic oxidation provided also important information about the reaction mechanism and then about the precursor of coke. Fig. 7 shows the product distribution profile of the DCA oxidation over H-BETA at 13,500 h^{-1}. Product distribution over H-ZSM-5 and H-MOR were reported previously by our research group.

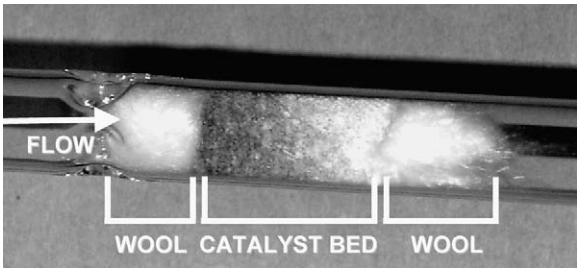

Fig. 6. Photograph of the coke profile in the spent catalytic bed (H-ZSM-5, 13,500 h^{-1}, 300 °C, 1000 ppm DCA).

Table 2
Coke contents with respect to the distance from the catalytic bed inlet (H-ZSM-5, 13,500 h^{-1}, 300 °C, 1 000 ppm DCA).

Segment of catalytic bed	Coke content (%)
Inlet	1.10
Centre	0.83
Outlet	0.33

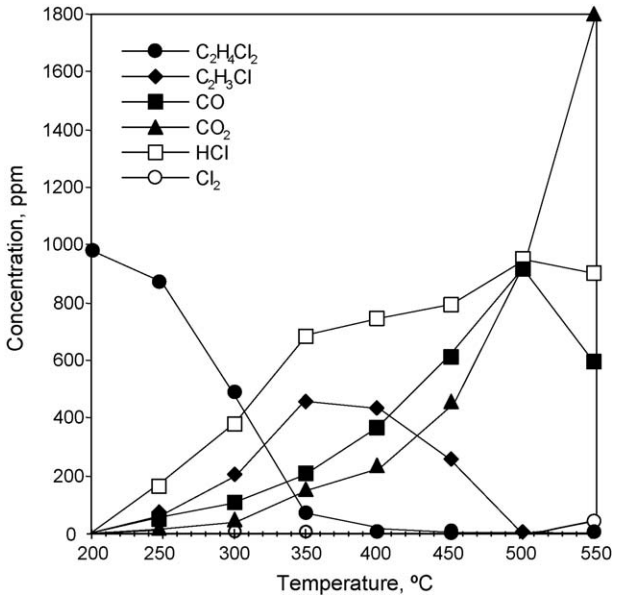

Fig. 7. Product distribution vs. temperature over H-BETA (13,500 h^{-1}, 1000 ppm DCA).

The main products were carbon monoxide, carbon dioxide and hydrogen chloride. Amounts of vinyl chloride were detected at 250 °C when DCE first started to react. The vinyl chloride concentration passed through a maximum at 350 °C. The presence of this intermediate suggested that the abstraction of HCl (dehydrochlorination) is the first step in the reaction process. Vinyl chloride, being stable, does not undergo further dehydrochlorination, and oxidized to CO, CO_2 and HCl. Ranging from 250 to 350 °C, the relation between the decline of DCE and the rise of vinyl chloride and HCl was almost linear. Neither CO and CO_2 appeared to be formed to low extent until vinyl chloride decomposition started at about 400 °C. Distribution profiles over H-ZSM-5 and H-MOR were similar and led to same conclusions [7].

These product distribution profiles suggested destruction of DCA occurs in two steps: first, hydrodechlorination to vinyl chloride (VC) via HCl elimination, which requires higher space time for subsequent oxidation to CO, CO_2 and HCl [39,40], as shown in the following reaction scheme:

$$C_2H_4Cl_2 \rightarrow C_2H_3Cl + HCl \quad (1)$$

$$C_2H_3Cl + \frac{3}{2}O_2 \rightarrow 2\,CO + HCl + H_2O \quad (2)$$

$$C_2H_3Cl + \frac{5}{2}O_2 \rightarrow 2\,CO_2 + HCl + H_2O \quad (3)$$

On acid catalysts, coking occurs rapidly from olefins or from reactants that undergo a rapid transformation into coke precursors, so in this reaction vinyl chloride is the olefinic intermediate, which initiates the reactions leading to coke formation. This high rate of coking from olefins is due to their rapid transformation through bimolecular reactions of oligomerization, alkylation and hydrogen transfer [33,34]. Therefore, in this case vinyl chloride may be the olefinic intermediate that starts the reaction leading to coke formation.

Taking up again discussion about coking mechanism, if we assume that deactivation is controlled by coke deposition, coke formation is probably the final step of a series-parallel reaction system as proposed in Eq. (4):

$$C_2H_4Cl_2 \rightarrow C_2H_3Cl \begin{cases} \nearrow CO, CO_2, HCl \\ \searrow CH_X \quad (Coke) \end{cases} \quad (4)$$

Increasing residence time, this reaction system can go to completion, so product formation is higher but also more coke is produced since both reactions are favoured with residence time [26,33].

Since coke is suggested to be formed by polimerisation of intermediate vinyl chloride, it is believed that coke composition would include chlorinated compounds. Table 3 presents the molecular formula and molecular weights of the components detected in the soluble coke. Only oxygenated aromatic compounds were identified and no chlorinated compounds were detected in the soluble fraction which means that chlorine could be combined to compounds with higher molecular weight. Unfortunately, it was impossible to establish the chemical composition of the insoluble fraction.

Table 3
Main components of the CH_2Cl_2 — soluble coke fraction.

Molecular weight	Formula
96	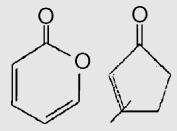
110	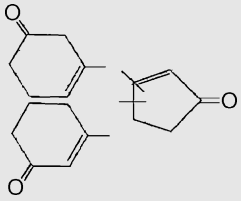
122	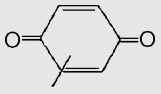
136	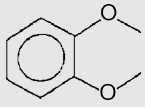
120	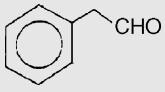
132	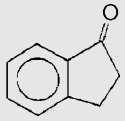
134	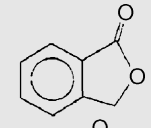

Table 3 (*Continued*)

Molecular weight	Formula
146	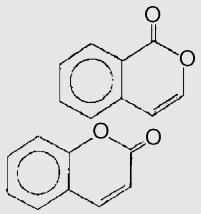
160	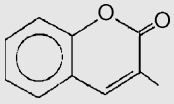
180	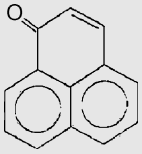
194	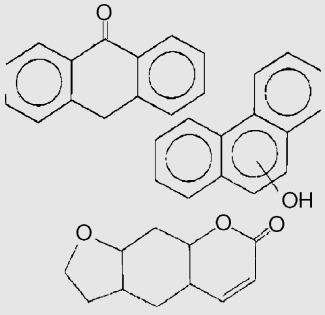

3.3. Effect of temperature on catalyst deactivation

The coking rate also depends on the reaction temperature. The Fig. 8 shows the activity drop of H-ZSM-5 zeolite as a function of reaction temperature at constant space velocity (13,500 h^{-1}) after 16 h of operation. It was observed that for temperatures below 290 °C the deactivation increased with temperature, whereas for temperatures above 290 °C deactivation decreased.

The change in the deactivation trend at 290 °C mentioned previously can be related to the fact that vinyl chloride, which polymerises rapidly into coke, increases with temperature up to 350 °C, but at the same time, the presence of oxygen in the feed involves coke burning over 290 °C, as confirmed by thermogravimetric analysis. These experimental results can also be explained by the series-parallel reaction system previously suggested to understand the effect of space velocity (Eq. (4)).

Comparing characterization results of used catalysts at 270 and 300 °C (Table 1), in can be noticed the loss of acidity is higher at 270 °C than at 300 °C in all the cases, possibly due to coke burning at higher temperatures.

3.4. Influence of HCl addition on zeolite deactivation

It is well known that the Al–O bonds of the zeolites used in the oxidation chlorinated VOCs can be attacked by the reaction product HCl [25], producing dealumination and consequently reducing its acidity and also its activity. Formed volatile $AlCl_3$ molecules (b.p. 178 °C) take away Al atoms from the zeolite and cause a partial collapse and blockage of the porous structure [41,42]. In order to understand the effect of HCl on the deactivation process, HCl (700 ppm) was added to the feed stream.

H-MOR suffered from severe deactivation when additional HCl was fed to the reaction environment. In the case of H-BEA deactivation was slightly increased with respect to HCl free feed, but deactivation was not enhanced when H-ZSM-5 was used, as observed in Fig. 9. Characterization results shown in Table 4, do not show loss of crystallinity due to dealumination, although $AlCl_3$ could not be detected by XRD analysis, since it is amorphous. BET area was also maintained in similar values. Loss of acidity was more severe in the presence of additional HCl (around 70–75%), and it was happened mainly over strong acid sites. However, there was no correlation between additional loss of activity (H-ZSM-5 < H-BEA < H-MOR) and loss of acidity: H-ZSM-5 (75%) > H-MOR (73%) > H-BEA (70%).

In the presence of additional HCl, coke was also formed, though in lower extent, especially over H-ZSM-5 and H-MOR. Then, according the activity and characterization results, it seems that though formation of coke was the main reason of zeolite deactivation, HCl produced in the reaction also reduced activity. As concluded by Zuhairi et al. [43] and Triantafillidis et al. [44], zeolites with high Si/Al ratio, like H-ZSM-5 (Si/Al = 25) and H-BEA (Si/Al = 12.5), showed higher resistance to HCl attack with respect to low Si/Al ratio like H-MOR (Si/Al = 6.5). H-MOR presents the highest proportion of Al atoms in its structure so it is more susceptible to be attacked by HCl.

3.5. Influence of H_2O addition on zeolite deactivation

In the real off-gas streams water vapour is also present, especially in the groundwater desorption units, so the presence of water in the feed stream (10,000 ppm) was considered.

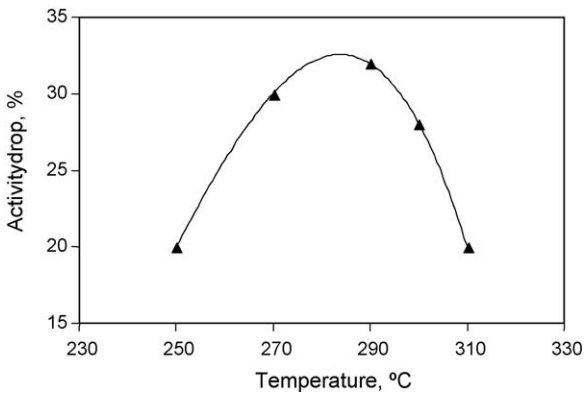

Fig. 8. Activity loss of H-ZSM-5 zeolite vs. temperature (13,500 h^{-1}, 1000 ppm DCA).

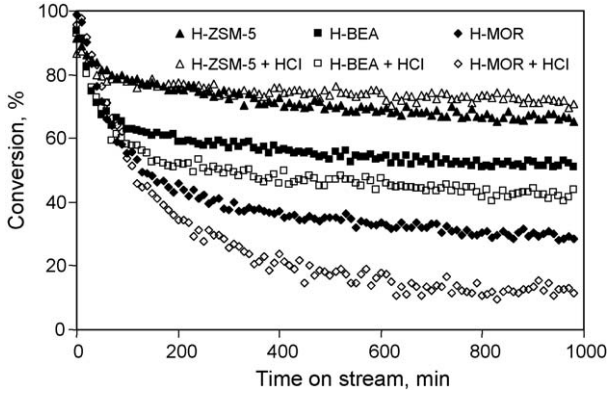

Fig. 9. Influence of the addition of 700 ppm HCl on the catalytic activity of H-zeolites (13,500 h^{-1}, 300 °C), as a function of time on stream.

Table 4
Characterisation of spent zeolites after addition of HCl and H_2O to the feedstream (13,500 h^{-1}, 300 °C, 1000 ppm DCA).

	S_{BET}, ($m^2\ g^{-1}$)	Weak acidity, (mmol $NH_3\ g^{-1}$)	Strong acidity, (mmol $NH_3\ g^{-1}$)	Total acidity, (mmol $NH_3\ g^{-1}$)	Crystallinity, (%)	Coke content, (%)
H-ZSM-5 (DCA)	336.7	0.098	0.163	0.261	100	2.3
H-ZSM-5 (DCA + HCl)	350.2	0.034	0.030	0.064	98	1.6
H-ZSM-5 (DCA + H_2O)	402.5	0.033	0.029	0.063	99	0.7
H-MOR (DCA)	322.4	0.208	0.238	0.446	99	2.2
H-MOR (DCA + HCl)	381.5	0.054	0.066	0.120	96	1.2
H-MOR (DCA + H_2O)	401.8	0.046	0.135	0.181	99	1.3
H-BEA (DCA)	400.5	0.104	0.158	0.261	89	3.4
H-BEA (DCA + HCl)	409.5	0.055	0.023	0.078	98	3.1
H-BEA (DCA + H_2O)	484.6	0.033	0.043	0.076	98	2.3

The conversion profiles along time on stream (Fig. 10) were the same type as in dry conditions. In the presence of water vapour, the initial conversion (fresh catalyst) of DCE was lower than conversion in dry conditions. The effect of water on the activity of fresh H-MOR zeolite resulted in a noticeable decrease in the DCE conversion, e.g. 16% lower, followed by fresh H-BEA (13% lower). On the contrary, the addition of water in the feed stream had a minimal effect on the conversion of fresh H-ZSM-5 (3%). The drop in activity of H-MOR (Si/Al = 6.5) is associated with the relatively strong hydrophilic character of aluminium-rich zeolites. This is in stark contrast with zeolites of high Si/Al ratio such as H-ZSM-5 (Si/Al = 25), which are markedly more hydrophobic, and therefore offer reduced sensibility to water inhibition of active sites. Then, the decrease in the activity can be explained by the competition between the reactant and water molecules for the adsorption on the hydroxyl groups of the zeolites [7,45], making some of them inactive for the desired reaction.

After 16 h of operation, the conversion drop with respect to initial conversion followed the same order as in dry conditions. H-ZSM-5 was the more resistant to deactivation, with a loss of 30%, followed by H-BEA (33% loss) and H-MOR (59% loss).

As reveal in Table 4, in humid conditions coke formation was considerably reduced in all the cases. Steam gasification is believed as the main mechanism by which coke is removed from the catalysts [46]. This fact was also evidenced by the change in the catalyst colour from dark to light brown. Then, conversion should improve, assuming pore plugging and catalytic site coverage are lower.

However, the presence of water vapour in the reaction environment also caused additional decrease in the acidity of three zeolites (Table 4), because of preferential adsorption of water molecules over acid sites. Then, it seems that the effect of competitive adsorption on the acid sites between H_2O and DCA molecules is stronger than the effect of lower coke formation.

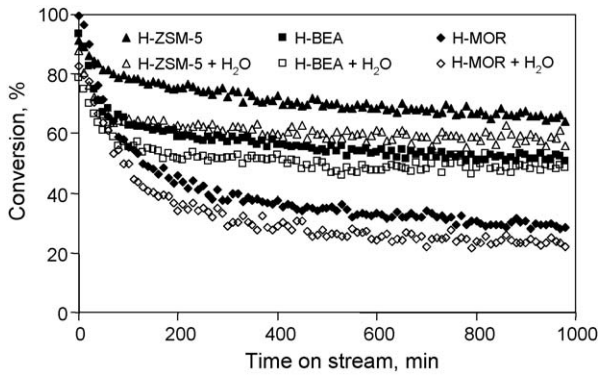

Fig. 10. Effect of the addition of 10,000 ppm H_2O on the catalytic activity of H-zeolites (13,500 h^{-1}, 300 °C), as a function of time on stream.

Moreover, the presence of water in the DCA decomposition changed markedly the reaction product distribution. Vinyl chloride formation was found to be significantly reduced over the three zeolites, and CO_2 selectivity was largely enhanced. Formation of Cl_2 was inhibited, due to the inversion of the Deacon reaction [40,45]. This effect on the selectivity was previously discussed elsewhere [7,47].

4. Conclusions

The deactivation of protonic zeolites in the catalytic oxidation of 1,2-dichloroethane was assessed. Both coke formation and HCl produced during reaction were found to be the reasons of zeolite deactivation.

The effect of coke formation on the stability of H-zeolites depends strongly on their pore channel system and of their total amount of acid sites. Coking causes zeolite pore plugging and catalytic site coverage and involves a loss in activity. H-ZSM-5 and H-BEA zeolites have an interconnected three-dimensional channel system, whereas H-MOR has a one-dimensional pore structure so pore blockage by coking is easier. H-ZSM-5 zeolite is the most stable zeolite due to its three-dimensional channel system, homogeneous channel size and interconnecting channels. The high Si/Al ratio of H-ZSM-5 also translates to lower acidity, thus lower coking trend and higher stability.

Attack of chloride formed during reaction also causes deactivation, specially in the zeolites with low Si/Al ratio. H-MOR presents the highest proportion of Al atoms in its structure so it is more susceptible to be attacked by HCl.

The deactivation degree increases with space velocity (lower residence times), therefore coke molecules result from species formed early in the reaction sequence. Then, a series-parallel mechanism for the formation of coke was proposed: DCA undergoes a hydrodechlorination into vinyl chloride intermediate, which can be transformed either to CO/CO_2 (and HCl) or polymerised to coke.

A temperature increase up to 290 °C improves vinyl chloride formation involving rapid polymerisation to coke (increase deactivation) but over this temperature coke molecules start burning due to the fed air and deactivation is reduced.

The addition of water to the feed reduced the formation of coke, but activity was reduced because of hydrophilic characteristic of zeolite leading to competition between the reactant and water molecules for the adsorption on the hydroxyl groups of the zeolites, making some of them inactive for the desired reaction. Then, the most hydrophobic zeolites (high Si/Al), such us H-ZMS-5, are most suitable to operate in presence of water.

Acknowledgements

The authors wish to thank to the Spanish Education and Science Ministry (Project CTQ2005-04383) for the financial support. One of

the authors (M.R.S.) acknowledges also to the Spanish Education and Science Ministry for the grant BES-2006-13729.

References

[1] European Envionment Agency (EEA), EMEP/CORINAIR Emission Inventory Guidebook – 2007, Technical report no. 16/2007, http://reports.eea.europa.eu/EMEP-CORINAIR5/, 2007.
[2] Directive 99/13/EC, EU Council Directive 1999/13/EC of 11 March 1999 on the limitation of emissions of volatile organic compounds due to the use of organic solvents in certain activities and installations, Retrieved 5 February 2001 from the World Wide Web: http://www.esig.otg/direng.htm.
[3] E.C. Moretti, Practical Solutions for Reducing Volatile Organic Compounds and Hazardous Air Pollutants, American Institute of Chemical Engineers, New York, 2001.
[4] H. Muller, B. Deller, B. Despeyroux, E. Peldszud, P. Kammerhofer, W. Kuhn, R. Spielmannleitner, M. Stoger, Catal. Today 17 (1993) 383–390.
[5] A.R. Gavaskar, B.C. Kim, S.H. Rodansky, S.K. Ong, E.G. Marchand, Environ. Prog. 14 (1995) 33–40.
[6] P. Hunter, S. Ted-Oyama, Control of Volatile Organic Compound Emissions: Conventional and Emerging Technologies, John Wiley & Sons, Inc, New York, 2000.
[7] R. López-Fonseca, A. Aranzabal, P. Steltenpohl, J.I. Gutiérrez-Ortiz, J.R. González-Velasco, Catal. Today 62 (2000) 367–377.
[8] R. López-Fonseca, B. de Rivas, J.I. Gutiérrez-Ortiz, A. Aranzabal, J.R. González-Velasco, Appl. Catal. B 41 (2003) 31–42.
[9] A.Z. Abdullah, M.Z. Abu Bakar, S. Bhatia, J. Hazard Mater. B129 (2006) 39–49.
[10] S. Scirè, S. Minicò, C. Crisafulli, Appl. Catal. B 45 (2003) 117–125.
[11] R. Hughes, Deactivation of Catalysts, Academic Press, London, 1984.
[12] J. Oudar, H. Wise, Deactivation and Poisoning of Catalysts, Marcel Dekker, New York, 1985.
[13] J.B. Butt, E.E. Petersen, Activation, Deactivation, and Poisoning of Catalysts, Academic Press, San Diego, 1988.
[14] C.H. Bartholomew, Appl. Catal. A 212 (2001) 17–60.
[15] J.A. Moulijn, A.E. van Diepen, F. Kapteijn, Appl. Catal. A 212 (2001) 17–60.
[16] R.J. Farrauto, C.H. Bartholomew, Fundamentals of Industrial Catalytic Processes, Chapman & Hall, Kluwer Academic Publishers, London, 1997.
[17] S. Bhatia, J. Beltramini, D.D. Do, Catal. Rev. Sci. Eng. 31 (1989) 431–480.
[18] C.H. Bartholomew, G.A. Fuentes, Catalyst deactivation, Study in Surface Science and Catalysis, vol. 111, Elsevier, Amsterdam, 1997.
[19] B Delmon, G.F. Froment, Catalyst deactivation, Study in Surface Science and Catalysis, vol. 126, Elsevier, Amsterdam, 1999.
[20] J.J. Spivey, J.B. Butt, Catal. Today 11 (1992) 465–500.
[21] C. Libanati, D.A. Ullenius, C.J. Pereira, Appl. Catal. B 15 (1998) 21–28.
[22] S. Vigneron, P. Deprelle, J. Hermia, Catal. Today 27 (1996) 229–236.
[23] S.K. Agarwal, J.J. Spivey, J.B. Butt, Appl. Catal. A 82 (1992) 259–275.
[24] R. Rachapudi, P.S. Chintawar, H.L. Greene, J. Catal. 185 (1999) 58–72.
[25] M. Guillemot, J. Mijoin, S. Mignard, P. Magnoux, Appl. Catal. A 327 (2007) 211–217.
[26] S. Chatterjee, H.L. Greene, Y.J. Park, Catal. Today 11 (1992) 569–596.
[27] C.V. Hidalgo, C.V.H. Itoh, T. Hattori, M. Niwa, Y. Hid Murakami, J. Catal 85 (1984) 362–369.
[28] C. Resini, T. Montanari, L. Nappi, G. Bagnasco, M. Turco, G. Busca, F. Bregani, M. Notaro, G. Rocchini, J. Catal. 214 (2003) 179–190.
[29] M. Niwa, N. Katada, Catal. Surv. Jpn. 1 (1997) 215–226.
[30] M. Guisnet, P. Magnoux, Appl. Catal. 54 (1989) 1–27.
[31] M. Guisnet, P. Magnoux, Appl. Catal. A 212 (2001) 83–96.
[32] A. Aranzabal, J.A. González-Marcos, J.L. Ayastuy, J.R. González-Velasco, Chem. Eng. Sci. 61 (2006) 3564–3576.
[33] E.G. Derouane, F. Lemos, C. Naccaciie, F. Ramoa-Riberio (Eds.), Zeolite Microporous Solids: Synthesis, Structure and Reactivity, Kulwer Academic Publishers, Dordrecht (The Netherlands), 1991, pp. 457–474.
[34] M. Guisnet, P. Magnoux, Stud. Surf. Sci. Catal. 88 (1994) 53–68.
[35] A. Zuhairi, M. Zailani, S. Bhatia, React. Kinet. Catal. Lett. 79 (2003) 143–148.
[36] R. López-Fonseca, J.I. Gutiérrez-Ortiz, M.A. Gutiérrez-Ortiz, J.R. Gonzalez-Velasco, J. Chem. Technol. Biotechnol. 78 (2002) 15–22.
[37] R. López-Fonseca, J.I. Gutiérrez-Ortiz, M.A. Gutiérrez-Ortiz, J.R. Gonzalez-Velasco, Recent Res. Devel. Catalysis. 2 (2003) 51–75.
[38] G.F. Froment, App. Catal. A 212 (2001) 117–128.
[39] M.R. Feijen-Jeurissen, J.J. Jorna, B.E. Nieuwenhuys, G. Sinquin, C. Petit, J.P. Hindermann, Catal. Today 54 (1999) 65–79.
[40] K. Ramanathan, J.J. Spivey, Combust. Sci. Tech. 63 (1989) 247–255.
[41] S. Karmakar, H.L. Greene, J. Catal. 148 (1994) 524–533.
[42] G.M. Bickle, T. Suzuki, Y. Mitarai, Appl. Catal. B: Environ. 4 (1994) 141–153.
[43] A.A. Zuhairi, M.A.B. Zailani, S. Bhatia, J. Hazard. Mater. B 129 (2006) 39–49.
[44] C.S. Triantafillidis, A.G. Vlessidis, L. Nalbandian, N.P. Evmiridis, Microporous Mesoporous Mater. 47 (2001) 369–388.
[45] R. López-Fonseca, J.I. Gutiérrez-Ortiz, J.R. Gonzalez-Velasco, Appl. Catal. A 271 (2004) 39–46.
[46] T.E. McMinn, F.C. Moates, J.T. Richardson, Appl. Catal. B 31 (2001) 93–105.
[47] R. López-Fonseca, A. Aranzabal, J.I. Gutiérrez-Ortiz, J.I. Álvarez-Uriarte, J.R. González-Velasco, Appl. Catal. B 30 (2001) 303–313.